PHYSICAL REVIEW B **96**, 201404(R) (2017)

Magnetic field inducing Zeeman splitting and anomalous conductance reduction of half-integer quantized plateaus in InAs quantum wires

Sadashige Matsuo,[1,*] Hiroshi Kamata,[1,2] Shoji Baba,[1] Russell S. Deacon,[3] Javad Shabani,[4,5] Christopher J. Palmstrøm,[4,6,7] and Seigo Tarucha[1,2,†]

[1]*Department of Applied Physics, University of Tokyo, 7-3-1 Hongo, Bunkyo-ku, Tokyo 113-8656, Japan*
[2]*Center for Emergent Matter Science, RIKEN, 2-1 Hirosawa, Wako-shi, Saitama 351-0198, Japan*
[3]*Advanced Device Laboratory, RIKEN, 2-1 Hirosawa, Wako-shi, Saitama 351-0198, Japan*
[4]*California NanoSystems Institute, University of California, Santa Barbara, California 93106, USA*
[5]*Center for Quantum Phenomena, Physics Department, New York University, New York, New York 10003, USA*
[6]*Electrical and Computer Engineering, University of California, Santa Barbara, California 93106, USA*
[7]*Materials Department, University of California, Santa Barbara, California 93106, USA*

(Received 4 September 2017; revised manuscript received 6 October 2017; published 7 November 2017)

We report on the magnetic field dependence of half-integer quantized conductance plateaus (HQPs) in InAs quantum wires. We observe HQPs at zero applied magnetic field in InAs quantum wires fabricated from a high-quality InAs quantum well. The application of in-plane magnetic field causes Zeeman splitting of the HQP features, indicating that the origin of the observed HQP is not spontaneous spin polarization. Additionally we observe that the conductance of the split HQPs decreases gradually as the in-plane magnetic field increases. We finally assume electron-electron interaction as a possible mechanism to account for the zero-field HQPs and the anomalous field dependence.

DOI: 10.1103/PhysRevB.96.201404

Since the seminal discovery of quantized conductance plateaus in quantum wires [1], anomalous conductance plateau quantization which is widely reported experimentally has been an intriguing topic in mesoscopic physics. This topic has been studied extensively from various aspects including the Tomonaga-Luttinger liquid (TLL), spontaneous spin polarization, and the Kondo effect. In the 1990s, it was reported that quantized plateau conductance of long GaAs quantum wires decreases at high temperature but maintains the plateau shape observed at lower temperatures [2–4]. This conductance reduction was explained as a property of the TLL, a one-dimensional electron liquid with electron-electron (e-e) interaction [5–8]. In 1996 another anomalous feature, the so-called 0.7 anomaly, was reported in GaAs quantum wires [9]. The anomaly appears as a shoulder or plateau-like structure at $0.7 \times 2e^2/h$ in addition to the quantized conductance plateaus. Although the 0.7 anomaly has been theoretically and experimentally studied [10–17], the origin remains a subject of debate.

Furthermore, anomalous conductance plateaus at half-integer multiples of quantized conductance (HQPs) have been observed even at zero magnetic field ($B = 0$ T) in GaAs quantum wires [18–20], carbon nanotubes [21], and InAs (InGaAs) quantum wires [22–24]. The observation of HQPs at $B = 0$ T is striking because we naively expect that spin states are degenerate, resulting in plateaus at multiples of $2e^2/h$, and therefore that steps quantized at e^2/h appear only in a spin-resolved quantum wire at finite magnetic field. HQPs were often reported in quantum wires with intrinsic or electric-field induced spin-orbit interaction (SOI). Therefore, the origin is sometimes interpreted as spin-related phenomena caused by SOI. Although there are several theoretical suggestions for the origin, such as spontaneous spin polarization [22,23,25], the Stern-Gerlach mechanism [24], a "spin-incoherent" Luttinger liquid (SILL) [26,27], and a nuclear spin helix (NSH) [20,28–30], the underlying physics is still controversial, much like the 0.7 anomaly. According to the spontaneous spin polarization (SSP) scenario, the lateral SOI and the e-e interaction invokes SSP resulting in the appearance of zero-field HQPs. The Stern-Gerlach mechanism (SG) suggests that the spin-filter effect invoked by SOI around the entrance of the wire results in different transmission probabilities, 0 and 1, for spin-up and spin-down electrons, respectively, resulting in the zero-field HQPs. Unlike the above two scenarios, SILL and NSH do not require SOI. SILL relies on a finite-temperature effect preventing the spin density wave mode from propagating and NSH relies on helix order of nuclear spins in a TLL. In experiments to feature the zero-field HQPs, the in-plane magnetic field dependence is critical because SSP and SG scenarios predict peculiar magnetic field dependence of HQPs that is not expected in conventional quantized conductance plateaus. The field dependence can also have important implications in recent studies on the spin effects in hybrid semiconductor-superconductor devices. Indeed application of in-plane magnetic field is a key ingredient for the creation of Majorana fermions in a combined system of a quantum wire with strong SOI and an s-wave superconductor [31–36].

Here we report on an experimental study of in-plane magnetic field dependence of the zero-field HQPs observed in InAs quantum wires fabricated from a quantum well. We discuss the validity of the most likely scenarios for the observed HQPs including SSP, SG, SILL, and NSH, but not all possible mechanisms. Note that we here study in detail the Zeeman effect because SSP, SG, SILL, and NSH predict different characteristic dependencies on B allowing the valid mechanism for HQPs to be identified.

*matsuo@ap.t.u-tokyo.ac.jp
†tarucha@ap.t.u-tokyo.ac.jp

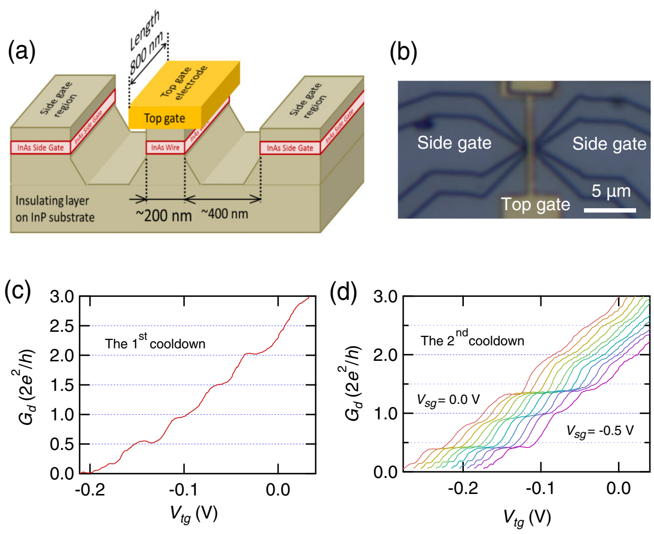

FIG. 1. (a) A schematic cross section of the fabricated quantum wire devices. (b) An optical image of the 0.8-μm-long wire device. The yellow part is a top-gate electrode and there are two side-gate electrodes. (c) The differential conductance G_d as a function of top-gate voltage V_{tg} obtained at $T = 1.5$ K in the first cool-down of the device is shown. There are 4 conductance plateaus observed at 0.5, 1.0, 1.5, and $2.0 \times 2e^2/h$. (d) G_d vs V_{tg} in the second cool-down of the device. Each curve is obtained at a different side-gate voltage V_{sg} between -0.5 V $< V_{sg} < 0.0$ V. The conductance of plateaus has a negligible dependence on V_{sg}.

Since InAs has a large g factor, resulting in a large Zeeman effect, and our quantum well has high mobility even at low carrier density, we clearly observe the Zeeman splitting of HQPs with an in-plane magnetic field, indicating that SSP does not occur. The observed magnetic field dependence is symmetric about the $B = 0$ T, indicating that SG is not the mechanism at play. Furthermore we found that increase of the in-plane magnetic field makes the conductance of HQPs smaller. We propose that these observed phenomena may be assigned to SILL in the quantum wire.

We fabricated quantum wire devices from a two-dimensional electron gas (2DEG) in InAs quantum wells [37–39]. The InAs well is 4 nm thick and the carrier density and mobility of the 2DEG are 3×10^{11} cm^{-2} and 30 m^2 V^{-1} s^{-1}, respectively. The mobility is remarkably high for such a low 2DEG density as compared to that used in most of the previous reports on HQPs. The e-e interaction plays an important role in the electron transport of quantum wires with a low carrier density, because the interaction strength is proportional to the carrier density n while the kinetic energy is proportional to n^2.

A schematic cross section of the fabricated quantum wire is shown in Fig. 1(a). In order to form a 200-nm-wide quantum wire with side-gate electrodes, the unnecessary parts of the 2DEG were etched away using a H_3PO_4-based etchant following the fabrication of a top-gate electrode (Ti 5 nm, Au 30 nm) which is used as a mask. In this Rapid Communication we focus on a wire of 0.8 μm length but to investigate the reproducibility we have also measured a 1.4-μm-long wire. Figure 1(b) shows an optical microscope picture of the 0.8-μm-long wire. The calculated mean-free path of the 2DEG is about 2.7 μm, which is sufficiently larger than the wire length. This means the wire transport is ballistic. We measure the differential conductance, $G_d = dI_d/dV_{sd}$ where I_d and V_{sd} are the drain current and source-drain voltage, respectively, using a four-terminal method to eliminate contributions from the conductance of the 2DEG in regions other than the wire. Measurements are performed in the temperature range of $T = 3.4$ K to 1.5 K using standard lock-in techniques. Due to restrictions of our setup, we warmed up the devices once when changing the orientation of the in-plane magnetic field. We applied in-plane magnetic fields parallel and perpendicular to the wire in the first and second cool-downs, respectively.

Figure 1(c) shows G_d as a function of the top-gate voltage V_{tg} at a side-gate voltage of $V_{sg} = -0.5$ V at $T = 1.5$ K in the first cool-down of the device. We applied the same negative gate voltage on both side-gate electrodes to suppress the possible surface accumulation states which remain as localized states on the edge and would work as scattering centers suppressing plateau conductance. Therefore, the negative V_{sg} reducing the localized states increases the conductance of some HQPs. In this figure we observe clear conductance plateaus at the half-quantized conductance, $G_d = 0.5$ and $1.5 \times 2e^2/h$. In contrast to previous reports, in which zero-field HQPs only appear at $G_d = 0.5 \times 2e^2/h$, we observe an additional plateau at $G_d = 1.5 \times 2e^2/h$. We note that the wire was unstable when sweeping V_{sg}, especially below -0.5 V, probably due to charging at the etched surface. Therefore, we fixed V_{sg} and varied the carrier density using V_{tg}. In the second cool-down, we observe similar HQPs in the range of -0.5 V $\leqslant V_{sg} \leqslant 0$ V as shown in Fig. 1(d). We note that HQPs are observed even at $V_{sg} = 0$ V. To characterize the wire properties, we measured temperature dependence [40] and bias voltage, V_{sd}, dependence [41], successfully demonstrating that the device shows the expected features of a one-dimensional electron system, excluding the anomalous plateau conductance. In these measurements, no evidence of the 0.7 anomaly and no apparent signatures from impurities are found [40,41]. The small structures around $0.25 \times 2e^2/h$ can be found in Fig. 1(c) and also in Fig. 1(d) with $V_{sg} = 0$ V. However the small structures vanish with $V_{sg} = -0.5$ V in Fig. 1(d) [and are not reproduced in the 1.4-μm-long wire as seen in Fig. 4(a)]. Therefore, we regard these structures as originating from the possible localized states of the accumulation layer and not from the same mechanism as HQPs.

Now we investigate the in-plane magnetic field dependence of the transconductance, G_{tr}, to study the mechanism generating zero-field HQPs, specifically whether the HQPs are related to the spin-related phenomena, SSP and SG. First, we applied an in-plane magnetic field parallel to the wire, $B_\parallel$. G_{tr} as a function of V_{tg} and $B_\parallel$ is plotted in Fig. 2(a). The bright regions (indicating low G_{tr}) correspond to the conductance plateaus, while the dark regions indicate the plateau transitions forming diamond-like features with white dashed lines as a guide for the eye. In this case, the diamond-like feature is explained by the Zeeman effect resolving the spin degeneracy as previously observed in p-type GaAs quantum wires under magnetic fields [42,43]. The Zeeman effect makes the dark regions split into two dark lines as the magnetic field increases from $B_\parallel = 0$ T. We can convert V_{tg} to an energy using the results of bias measurement [41] allowing the evaluation of

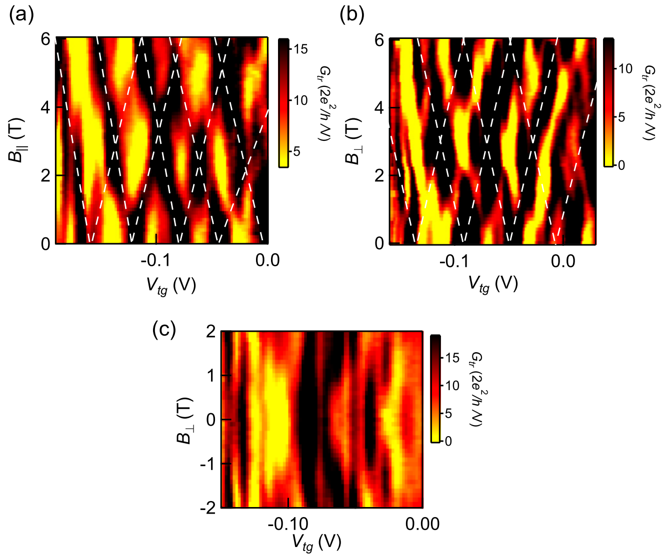

FIG. 2. (a) G_{tr} as a function of V_{tg} and $B_{\parallel}$. Zeeman splitting of the subbands is clearly seen as diamond-shaped structures, indicated with white dashed lines. (b) G_{tr} as a function of V_{tg} and $B_{\perp}$. The field dependence is very similar to the dependence in the $B_{\parallel}$ case. (c) G_{tr} as a function of V_{tg} and $B_{\perp}$ around $B_{\perp} = 0$ T. The observed structures are symmetric about $B_{\perp} = 0$ T.

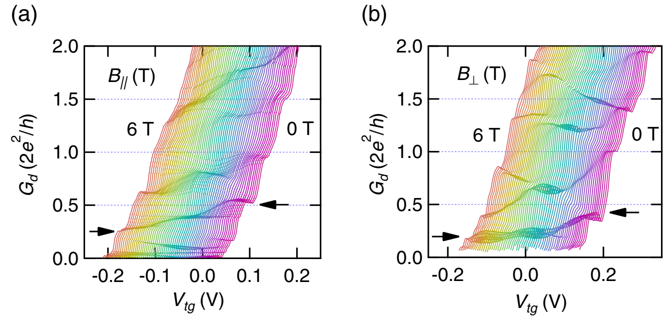

FIG. 3. (a) G_d vs V_{tg} obtained at different $B_{\parallel}$ are shown. The horizontal axis shows the result at 6 T and the other results are incrementally shifted by 0.004 V for clarity. The lowest plateau conductance is less than $0.5 \times 2e^2/h$ and the plateau conductance gradually decreases as $B_{\parallel}$ increases. (b) G_d vs V_{tg} obtained at different $B_{\perp}$ are shown. The horizontal axis shows the result at $B_{\perp} = 6$ T and the other results are incrementally shifted by 0.005 V for clarity. The main features are the same as obtained in the $B_{\parallel}$ case.

the $g$factor from the splitting of the dark lines, resulting in 5.1 for the $0.5 \times 2e^2/h$ plateau. This value is consistent with that previously reported for InAs systems (quantum dot, $3 \sim 9$; bulk, 14) [37–40]. The present observation clearly indicates that the subbands are spin degenerate at $B_{\parallel} = 0$ T and the degeneracy is lifted by application of $B_{\parallel}$.

To further confirm the Zeeman effect, we measured G_{tr} in the presence of an in-plane magnetic field $B_{\perp}$ perpendicular to the wire, and plot the obtained result in Fig. 2(b). As expected from the $B_{\parallel}$ experiment of Fig. 2(a), we observe a diamond-shaped G_{tr} pattern produced by the Zeeman effect. The g factor derived from the white dashed lines which split from the transition between the 0.5 and $1 \times 2e^2/h$ plateaus at 0 T is 5.9, consistent with that obtained from the $B_{\parallel}$ dependence. This consistency is also reported in the (In, Ga)As quantum point contact [44,45]. There is no qualitative difference between the $B_{\perp}$ and $B_{\parallel}$ measurements as shown in Figs. 2(a) and 2(b). In addition, we closely measured the $B_{\perp}$ dependence of the G_{tr} vs V_{tg} around $B_{\perp} = 0$ T shown in Fig. 2(c). All of the main features in Fig. 2(c) are symmetric about $B_{\perp} = 0$ T.

We now consider the plateau conductance in finite magnetic fields. Figure 3(a) shows G_d at $V_{sd} = 0$ V as a function of V_{tg} measured for various values of $B_{\parallel} < 6$ T in panel (c) and $B_{\perp} < 6$ T in panel (d). Surprisingly the conductance of the lowest plateau at high magnetic fields is smaller than e^2/h, as highlighted by arrows on the $B = 6$ T traces in both figures. The conductance gradually decreases, starting from a value of about e^2/h (indicated by arrows on the $B = 0$ T traces) as the magnetic field increases. These anomalous magnetic field dependencies are obtained for the conductance measured at $V_{sd} = 0$ V, so the mechanism is different from the bias-induced plateaus discussed in the Supplemental Material [41].

Finally we measure a longer wire device (1.4 μm length) to check the reproducibility of the HQP data. Figure 4(a) indicates the G_d vs V_{tg} obtained at $T = 1.5$ K in the case of $V_{sg} = 0$, -2.0, and -4.0 V, respectively. The zero-field HQP appears at $G_d = 0.5 \times 2e^2/h$ in addition to the quantized plateau at $G_d = 2e^2/h$. Figure 4(b) shows G_{tr} vs V_{tg} with $V_{sg} = -2.0$ V measured as a function of $B_{\parallel}$ and V_{tg}. From this dependency, we can estimate the Landé g factor of 5.6, which is consistent with the estimated value in the 0.8-μm-long wire devices. Figure 4(c) shows the G_d vs V_{tg} at $0\,\text{T} \leqslant B_{\parallel} \leqslant 8$ T. In Fig. 4(c) G_d of the plateaus at finite magnetic fields as indicated by two arrows for 4 and 8 T is smaller than that at 0 T. The main

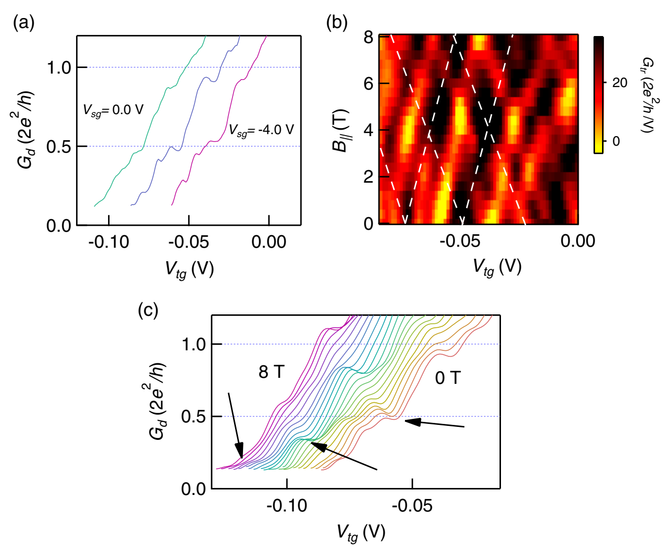

FIG. 4. (a) G_d vs V_{tg} of the 1.4-μm-long wire device with different V_{sg}. Plateaus at 0.5 and $1.0 \times 2e^2/h$ are observed. (b) Transconductance as a function of $B_{\parallel}$ and V_{tg}. Diamond structure originating from the Zeeman splitting is found as similar to the case of the 0.8-μm-long wire. (c) G_d vs V_{tg} obtained at $0\text{ T} < B_{\parallel} < 8$ T. The horizontal axis shows the result at $B_{\parallel} = 0$ T and the other results are incrementally shifted by -0.002 V for clarity. The plateau conductance at finite magnetic field is lower than the $2e^2/h$, as highlighted by arrows indicating the plateau at 8 T, 4 T, and 0 T.

features of HQPs observed in the 0.8-μm-length wire device are all reproduced in the longer wire device, and therefore we conclude that this anomalous conductance reduction observed at high fields is not due to impurities or roughness in the wires but an intrinsic phenomenon.

We first discuss the observed features in the context of predictions from SSP and SG. Both proposed mechanisms are based on strong SOI predicted to generate HQPs previously observed in InAs or InGaAs quantum wires. First, SSP is not suitable to explain our results, especially the Zeeman splitting or the zero-field HSQ features. The observed Zeeman splitting is strong evidence that HQPs consist of spin-degenerated subbands. Additionally, the proposed spin polarization mechanism requires a lateral electric field induced by asymmetry in the side gating, whereas we observe the zero-field HQPs even at $V_{sg} = 0$ V. SG also does not hold for our results. In this mechanism, the subbands are spin degenerated but the transmittance of the wire depends on the spin direction perpendicular to the plane of the injected electrons. Therefore it is expected that the subband energy of HQP decreases when $B_\perp$ is applied in the same direction as the injected electron spin, while the energy increases when $B_\perp$ is applied in the opposite direction. The $B_\perp$ dependence in the dc bias measurement should be asymmetry about $B_\perp = 0$ T. However, we do not recognize any such asymmetry as shown in Fig. 2(c).

For several reasons we conclude that HQPs and the anomalous reduction of the HQP conductance with magnetic field arise from e-e interaction. First, there is no significant difference between the $B_\parallel$ dependence and the $B_\perp$ dependence, in contrast to expectations for spin-related phenomena. Second, plateau conductance significantly below e^2/h is difficult to explain with a single-electron picture which would result in e^2/h as the lowest plateau conductance in the ballistic transport regime. At least, we can conclude that the magnetic field dependencies are not explained by SSP and SG, namely the mechanisms with strong SOI in the wire. Therefore, we suspect that the observed features are assigned to SILL or NSH, the mechanism induced by the e-e interaction (related phenomena to TLL). However SILL and NSH cannot be assigned to the anomalous conductance reduction induced by the in-plane magnetic fields. In order to completely reveal the mechanism, further theoretical and experimental efforts are required. For example, an experimental study of wires formed by split-gate and center-gate electrodes in order to reveal the carrier density dependence may be significant to reveal the mechanism.

In summary, we experimentally studied the electron transport in InAs quantum wires and its in-plane magnetic field dependence. Using a high-quality InAs quantum well with large g factor, we observed HQPs and the in-plane magnetic field dependence of the Zeeman splitting, indicating that HQPs are formed from spin-degenerated subbands. In addition, we discovered that the HQP plateau conductance decreases as the in-plane magnetic field increases. These results are inconsistent with predictions from the previously proposed mechanisms such as the spontaneous spin polarization and the Stern-Gerlach mechanism. Though not clarified we finally assume the e-e interaction as a possible mechanism to account for the observed HQP feature.

We greatly thank Yasuhiro Tokura, Makoto Kohda, Jelena Klinovaja, and Peter Stano for fruitful discussions. This work was partially supported by a Grant-in-Aid for Young Scientific Research (A) (Grant No. JP15H05407), Grant-in-Aid for Scientific Research (A) (Grant No. JP16H02204), Grant-in-Aid for Scientific Research (S) (Grant No. JP26220710), JSPS Research Fellowship for Young Scientists (Grant No. JP14J10600), and the JSPS Program for Leading Graduate Schools (MERIT) from JSPS, Grants-in-Aid for Scientific Research on Innovative Area "Nano Spin Conversion Science" (Grants No. JP15H01012 and No. JP17H05177) and a Grant-in-Aid for Scientific Research on Innovative Area "Topological Materials Science" (Grant No. JP16H00984) from MEXT, JST CREST (Grant No. JPMJCR15N2), and the Murata Science Foundation.

[1] B. J. van Wees, H. van Houten, C. W. J. Beenakker, J. G. Williamson, L. P. Kouwenhoven, D. van der Marel, and C. T. Foxon, Phys. Rev. Lett. **60**, 848 (1988).

[2] S. Tarucha, T. Honda, and T. Saku, Solid State Commun. **94**, 413 (1995).

[3] A. Yacoby, H. L. Stormer, N. S. Wingreen, L. N. Pfeiffer, K. W. Baldwin, and K. W. West, Phys. Rev. Lett. **77**, 4612 (1996).

[4] E. Levy, A. Tsukernik, M. Karpovski, A. Palevski, B. Dwir, E. Pelucchi, A. Rudra, E. Kapon, and Y. Oreg, Phys. Rev. Lett. **97**, 196802 (2006).

[5] S. Tomonaga, Prog. Theor. Phys. **5**, 544 (1950).

[6] C. L. Kane and M. P. A. Fisher, Phys. Rev. B **46**, 15233 (1992).

[7] M. Ogata and H. Fukuyama, Phys. Rev. Lett. **73**, 468 (1994).

[8] D. L. Maslov, Phys. Rev. B **52**, R14368(R) (1995).

[9] K. J. Thomas, J. T. Nicholls, M. Y. Simmons, M. Pepper, D. R. Mace, and D. A. Ritchie, Phys. Rev. Lett. **77**, 135 (1996).

[10] K. J. Thomas, J. T. Nicholls, N. J. Appleyard, M. Y. Simmons, M. Pepper, D. R. Mace, W. R. Tribe, and D. A. Ritchie, Phys. Rev. B **58**, 4846 (1998).

[11] A. Kristensen, H. Bruus, A. E. Hansen, J. B. Jensen, P. E. Lindelof, C. J. Marckmann, J. Nygård, C. B. Sørensen, F. Beuscher, A. Forchel, and M. Michel, Phys. Rev. B **62**, 10950 (2000).

[12] D. J. Reilly, G. R. Facer, A. S. Dzurak, B. E. Kane, R. G. Clark, P. J. Stiles, R. G. Clark, A. R. Hamilton, J. L. O'Brien, N. E. Lumpkin, L. N. Pfeiffer, and K. W. West, Phys. Rev. B **63**, 121311(R) (2001).

[13] S. M. Cronenwett, H. J. Lynch, D. Goldhaber-Gordon, L. P. Kouwenhoven, C. M. Marcus, K. Hirose, N. S. Wingreen, and V. Umansky, Phys. Rev. Lett. **88**, 226805 (2002).

[14] L. P. Rokhinson, L. N. Pfeiffer, and K. W. West, Phys. Rev. Lett. **96**, 156602 (2006).

[15] L. DiCarlo, Y. Zhang, D. T. McClure, D. J. Reilly, C. M. Marcus, L. N. Pfeiffer, and K. W. West, Phys. Rev. Lett. **97**, 036810 (2006).

[16] F. Bauer, J. Heyder, E. Schubert, D. Borowsky, D. Taubert, B. Bruognolo, D. Schuh, W. Wegscheider, J. v. Delft, and S. Ludwig, Nature (London) **501**, 73 (2013).

[17] M. J. Iqbal, R. Levy, E. J. Koop, J. B. Dekker, J. P. de Jong, J. H. M. van der Velde, D. Reuter, A. D. Wieck, R. Aguado, Y. Meir, and C. H. van der Wal, Nature (London) **501**, 79 (2013).
[18] R. Crook, J. Prance, K. J. Thomas, S. J. Chorley, I. Farrer, D. A. Ritchie, M. Pepper, and C. G. Smith, Science **312**, 1359 (2006).
[19] W. K. Hew, K. J. Thomas, M. Pepper, I. Farrer, D. Anderson, G. A. C. Jones, and D. A. Ritchie, Phys. Rev. Lett. **101**, 036801 (2008).
[20] C. P. Scheller, T.-M. Liu, G. Barak, A. Yacoby, L. N. Pfeiffer, K. W. West, and D. M. Zumbühl, Phys. Rev. Lett. **112**, 066801 (2014).
[21] M. J. Biercuk, N. Mason, J. Martin, A. Yacoby, and C. M. Marcus, Phys. Rev. Lett. **94**, 026801 (2005).
[22] P. Debray, S. M. S. Rahman, J. Wan, R. S. Newrock, M. Cahay, A. T. Ngo, S. E. Ulloa, S. T. Herbert, M. Muhammad, and M. Johnson, Nat. Nanotechnol. **4**, 759 (2009).
[23] J. Wan, M. Cahay, P. Debray, and R. Newrock, Phys. Rev. B **80**, 155440 (2009).
[24] M. Kohda, S. Nakamura, Y. Nishihara, K. Kobayashi, T. Ono, J.-i. Ohe, Y. Tokura, T. Mineno, and J. Nitta, Nat. Commun. **3**, 1082 (2012).
[25] A. T. Ngo, P. Debray, and S. E. Ulloa, Phys. Rev. B **81**, 115328 (2010).
[26] K. A. Matveev, Phys. Rev. B **70**, 245319 (2004).
[27] G. A. Fiete, Rev. Mod. Phys. **79**, 801 (2007).
[28] B. Braunecker, P. Simon, and D. Loss, Phys. Rev. Lett. **102**, 116403 (2009).
[29] B. Braunecker, P. Simon, and D. Loss, Phys. Rev. B **80**, 165119 (2009).
[30] B. Braunecker, G. I. Japaridze, J. Klinovaja, and D. Loss, Phys. Rev. B **82**, 045127 (2010).
[31] L. Fu and C. L. Kane, Phys. Rev. Lett. **100**, 096407 (2008).
[32] M. Z. Hasan and C. L. Kane, Rev. Mod. Phys. **82**, 3045 (2010).
[33] V. Mourik, K. Zuo, S. M. Frolov, S. R. Plissard, E. P. A. M. Bakkers, and L. P. Kouwenhoven, Science **336**, 1003 (2012).
[34] A. Das, Y. Ronen, Y. Most, Y. Oreg, M. Heiblum, and H. Shtrikman, Nat. Phys. **8**, 887 (2012).
[35] L. P. Rokhinson, X. Liu, and J. K. Furdyna, Nat. Phys. **8**, 795 (2012).
[36] S. M. Albrecht, A. P. Higginbotham, M. Madsen, F. Kuemmeth, T. S. Jespersen, J. Nygard, P. Krogstrup, and C. M. Marcus, Nature (London) **531**, 206 (2016).
[37] See Supplemental Material at http://link.aps.org/supplemental/10.1103/PhysRevB.96.201404 for stack materials of the InAs quantum well wafer .
[38] J. Shabani, S. Das Sarma, and C. J. Palmstrøm, Phys. Rev. B **90**, 161303 (2014).
[39] J. Shabani, A. P. McFadden, B. Shojaei, and C. J. Palmstrøm, Appl. Phys. Lett. **105**, 262105 (2014).
[40] See Supplemental Material at http://link.aps.org/supplemental/10.1103/PhysRevB.96.201404 for temperature dependence of the zero-field HQPs .
[41] See Supplemental Material at http://link.aps.org/supplemental/10.1103/PhysRevB.96.201404 for bias voltage dependence of the zero-field HQPs .
[42] Y. Komijani, M. Csontos, I. Shorubalko, U. Zülicke, T. Ihn, K. Ensslin, D. Reuter, and A. D. Wieck, Europhys. Lett. **102**, 37002 (2013).
[43] F. Nichele, S. Chesi, S. Hennel, A. Wittmann, C. Gerl, W. Wegscheider, D. Loss, T. Ihn, and K. Ensslin, Phys. Rev. Lett. **113**, 046801 (2014).
[44] T. P. Martin, A. Szorkovszky, A. P. Micolich, A. R. Hamilton, C. A. Marlow, H. Linke, R. P. Taylor, and L. Samuelson, Appl. Phys. Lett. **93**, 012105 (2008).
[45] T. P. Martin, A. Szorkovszky, A. P. Micolich, A. R. Hamilton, C. A. Marlow, R. P. Taylor, H. Linke, and H. Q. Xu, Phys. Rev. B **81**, 041303 (2010).